BOREAL ENVIRONMENT RESEARCH 16: 15–35
ISSN 1239-6095 (print) ISSN 1797-2469 (online)

Helsinki 28 February 2011

Geographical origin of aerosol particles observed during the LAPBIAT measurement campaign in spring 2003 in Finnish Lapland

Marko Kaasik[1)], Mikhail Sofiev[2)], Marje Prank[2)], Taina Ruuskanen[3)], Jaakko Kukkonen[2)], Urmas Hõrrak[1)] and Markku Kulmala[3)]

[1)] *Institute of Physics, University of Tartu, Ülikooli 18, EE-50090 Tartu, Estonia*
[2)] *Finnish Meteorological Institute, P.O. Box 503, FI-00101 Helsinki, Finland*
[3)] *Department of Physics, P.O. Box 64, FI-00014 University of Helsinki, Finland*

Received 14 Dec. 2009, accepted 9 Apr. 2010 (Editor in charge of this article: Veli-Matti Kerminen)

Kaasik, M., Sofiev, M., Prank, M., Ruuskanen, T., Kukkonen, J., Hõrrak, U. & Kulmala, M. 2011: Geographical origin of aerosol particles observed during the LAPBIAT measurement campaign in spring 2003 in Finnish Lapland. *Boreal Env. Res.* 16: 15–35.

A modelling analysis of observations of aerosol concentrations during the LAPBIAT measurement campaign is presented and possible sources of the aerosols and their precursors are discussed. The LAPBIAT measurement campaign at the SMEAR I station at Värriö in eastern Lapland took place from 26 April to 11 May 2003 and registered a series of particle formation events. The SILAM model was applied in adjoint (inverse) mode for back-tracing the air masses observed during several selected episodes. It was also applied in forward mode using the EMEP sulphur emission data in order to qualitatively evaluate the contribution of anthropogenic sulphur to the corresponding events. As shown by adjoint simulations, the air masses corresponding to the observed peaks of concentrations of the nucleation-size aerosol often originated from areas different from the source regions responsible for the observed aged pollution plumes. We examined the origins of air masses during three nucleation events registered during the Värriö campaign. Observations of the first nucleation event were interrupted when polluted plume from the Nikel metallurgy plant (Russia) was transported to the site, replacing the cleaner air masses with the on-going particle formation. The second (most intensive) event occurred in the air that was transported for substantial distances over the central part of Finland in prevailing dry and relatively warm conditions. Since such conditions correspond to large biogenic VOC emissions, one can expect a major contribution of these species in the observed event. During the third episode, the air masses were transported directly from the Arctic Sea, thus suggesting a significant impact of marine aerosols. Also, three episodes with elevated concentrations of accumulation and coarse range particles were found. According to adjoint simulations, urban and industrial emissions were responsible for these events.

Introduction

A series of studies during the last decade have shown that aerosol formation can take place in substantially different environments and is much more common than has previously been known (e.g. Kulmala *et al*. 2004a, 2008). It has also been shown that the formation events and subsequent chemical and physical reactions of ageing of pollutants last for at least several hours. However, most of observations and process studies of aerosol formation are based on the homogeneous-volume assumption, i.e., the properties of the passing air mass are assumed to be constant during the event (Kulmala *et al*. 1995).

The validity of such an assumption depends on several factors. Thus, the meteorological conditions substantially vary on a time-scale of hours and can sometimes undergo sharp changes at a time scale of tens of minutes. Clearly, the chemical composition of the plumes also alters when these are transported over source and sink areas. Species can be scavenged by precipitation, which can result in sharp gradients of concentrations in both time and space. Therefore, short term observations alone at any single location cannot provide sufficient information to restore the history of the transformations that took place in the observed air volume even in recent past. This can potentially lead to misinterpretations of aerosol dynamics and chemistry.

There are several categories of mathematical methods for describing the atmospheric transport and transformations that are used for the analysis and interpretation of the observed pollutant concentrations. These can be broadly categorised to backward trajectories, conventional atmospheric dispersion modelling, and adjoint (i.e. inverse) modelling.

i. The most widespread approach is based on qualitative consideration of backward trajectories using an appropriate model, such as, e.g., the HYSPLIT trajectory model (Draxler and Rolph 2003). The analysis is commonly based on meteorological fields computed by numerical weather prediction models, and a Lagrangian advection algorithm. The models can be used to evaluate the trajectories backward in time, arriving at the monitoring site at the moment when a particular measured value is recorded. Interpretation of the results is usually qualitative (e.g. Skjøth *et al*. 2007, Barletta *et al*. 2009), but sometimes quantitative analysis can be undertaken (Kulmala *et al*. 2000, Sogacheva *et al*. 2005, 2007, Heo *et al*. 2009).
ii. The second category of methods is based on modelling of the atmospheric transport and diffusion forward in time, followed by the model-measurement comparison, sometimes accompanied by sensitivity studies (e.g. Stern *et al*. 2008). Systematic discrepancies of model predictions and measured values are then analysed and attributed to either the deficiency of the applied model(s), or to specific processes, such as misinterpreted meteorological developments, missing or inaccurate emission data, etc.
iii. The third method has been used for local case studies for several years — so-called footprint estimation on the basis of the adjoint dispersion equation (e.g. Rannik *et al*. 2003, Kuparinen 2006, Kuparinen *et al*. 2007a, 2007b, Vesala *et al*. 2008) and in the source apportionment of greenhouse gas emissions (Bergamaschi *et al*. 2005). The methodology has recently also been adopted to the analysis of regional air quality (e.g. Saarikoski *et al*. 2007, Kaasik *et al*. 2008, Prank *et al*. 2008) and the dispersion of allergenic pollen (Sofiev *et al*. 2006a, 2006c, 2006d, Siljamo *et al*. 2008). The method is based on the numerical solution of the adjoint dispersion equation (*see* the background in Marchuk 1982).

The idea of the adjoint dispersion method is to explicitly compute the sensitivity of the observed values to emission fluxes, chemical transformations and meteorological processes that can affect the particular observation. This approach is directly associated to variational data assimilation methods, which are more and more widely used in both meteorological and dispersion applications (Unden 2002, Kalnay 2003, Fisher and Lary 1995, Elbern *et al*. 1997, 1999, 2007, Vira 2008). Essentially, the footprint evaluation is the first half of the first-iteration cycle of the 4D-VAR (four-dimensional variational data assimilation), which is interpreted by

4D-VAR as a gradient of the cost function (usually, the root-mean-square-error of the model-measurement scatter plot) with regard to emissions, initial conditions, or model parameters.

In comparison with the first two approaches, the adjoint dispersion formalism allows a much more accurate and direct quantitative estimation of the source regions that affect a particular observation. However, the adjoint modelling is currently rarely applied to the analysis of the observations, except for in the local footprint computations (Vesala *et al*. 2008). This is probably due to the apparent complexity of the approach and its relatively higher computational and development costs as compared with, e.g., the qualitative analysis with backward trajectories.

The goal of the current study is to analyse the results of the observational campaign at the station of Värrio (Ruuskanen *et al*. 2007) by means of the regional-scale footprint computations, and highlight the possible source regions that contributed to the numerous nucleation events during April and May 2003. In particular, we aim at explaining the characteristics of the selected nucleation events, which were in some cases strongly disturbed by external impacts. To the best of our knowledge, such an analysis of the sources of the aerosol formation events using adjoint dispersion modelling has not been published previously. The combined usage of forward and adjoint dispersion computations is also scarce in the literature, except for the above-mentioned data assimilation studies.

Fig. 1. Locations of the measurement site (cross), major industrial pollution sources (metal smelters etc., dots), and major cities (circles).

Experimental data

The field experiments were carried out at the SMEAR I site (Station for Measuring Forest Ecosystem–Atmosphere Relation, 67°46´N, 29°35´E) (Hari *et al*. 1994), located in Värriö nature park in eastern Lapland, less than 10 km from the border with Russia and 100–200 km away from major pollution sources at the Kola Peninsula (Fig. 1).

The campaign included measurements of aerosol particle size distributions with EAS (electric aerosol spectrometer, Tammet *et al*. 2002) from 28 April to 11 May 2003. Detailed description of campaign design and results is reported by Ruuskanen *et al*. (2007). Atmospheric concentrations of trace gases including SO_2, O_3 and NO_x were also measured. The EAS can be used to measure aerosol size distribution in the aerodynamic diameter range of 3 nm–10 μm with spectral resolution of 8 fractions per decade (28 fractions in total). The wide range of measurable particle sizes is an advantage of EAS as compared with other equipment used at SMEAR I (*see* Ruuskanen *et al*. 2007). In order to compare the measured data with the model predictions, the EAS fractions were grouped into four aerosol modes (Table 1; *see* also e.g. Mäkelä *et al*. 2000, Pirjola *et al*. 2003).

Time series of the concentrations of all modes exhibit narrow sharp peaks and relatively long time intervals with much lower values (Fig. 2). We assumed that these low levels represent the background concentrations (Table 1, second column from right). Note that number concentrations (rightmost column) are only approximates and given for easier understanding, due to large size range the relation between mass and number concentrations is far

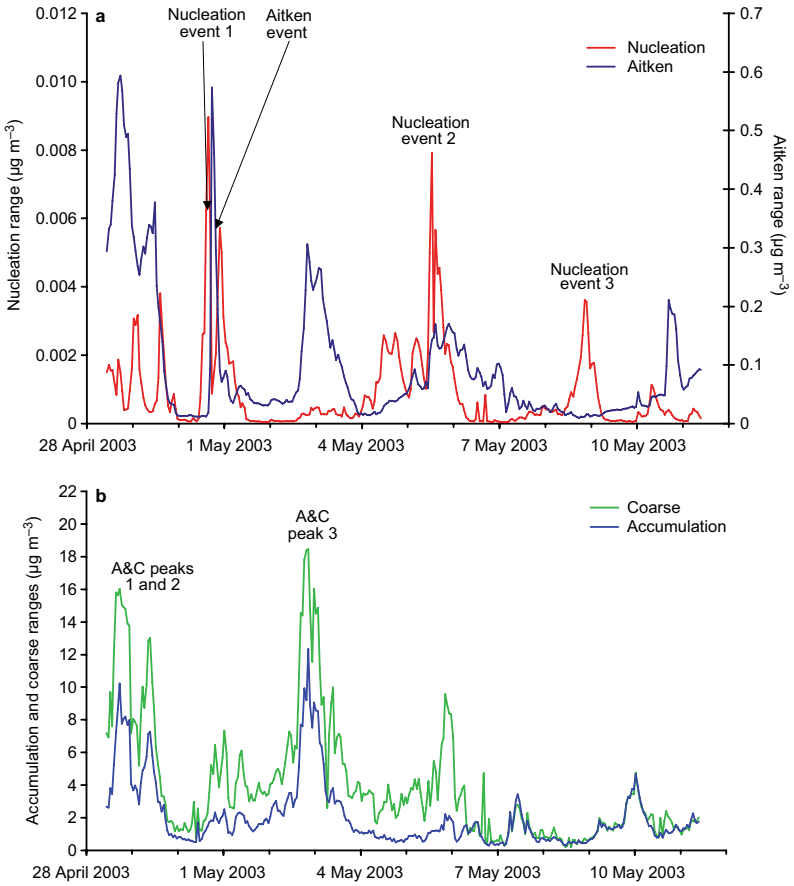

Fig. 2. Hourly average mass concentrations of aerosol particles in (**a**) nucleation and Aitken, and (**b**) accumulation and coarse modes, measured by the EAS during the campaign at the station of Värriö in April–May 2003. The legends in the figure show the numbering of the peaks, as used in the text.

from functional dependence. Background levels were subtracted from the total measured concentrations for inverse model runs. If subtraction resulted in negative values (i.e. concentrations were even smaller than the typical background), these were replaced with zeroes. The idea of such processing was to enhance the sensitivity of model to strong sources, which presumably cause the highest concentrations. It was easier to visually distinguish the footprints of concentration peaks in the model output, after the background produced by diffuse sources was eliminated. The effect of this manipulation to the peak concentrations is negligible, because these are several times higher than background.

Table 1. Aerosol size ranges distinguished in the size distributions during the Värriö campaign. Maximum background concentrations of aerosol particles have been defined in the text.

Size range	Diameter (nm)		Number of EAS fractions	Estimated maximum background concentration	
	min.	max.		μg m^{-3}	approx. particles (cm^{-3})
Nucleation	3	24	7	0.001	1000
Aitken	24	100	5	0.05	1000
Accumulation	100	1000	8	2	400
Coarse	1000	10000	8	4	2

Modelling methods

The atmospheric dispersion and numerical weather prediction models

The variant of the SILAM model used in this study is based on a Lagrangian particle Monte-Carlo dynamics. The model has been developed at the Finnish Meteorological Institute and has been validated against the meso-scale European Tracer Experiment (ETEX) (Sofiev *et al*. 2006b), the results of various field measurement campaigns, and the long-term air quality observations of EMEP (Sofiev *et al*. 2006b, 2006c). For aerosol, SILAM considers advective and turbulent transport, and dry (including size-dependent sedimentation) and wet deposition.

The SILAM model has two modes of operation: forward and adjoint (Sofiev *et al*. 2006d). In the forward mode, the input data contain emissions from specified sources, meteorological input data produced by numerical weather prediction models, land use data and other data. The output of the forward simulation consists of the four-dimensional (4-D) fields of concentrations (i.e. 3-D spatial patterns and their temporal evolutions) and 3-D dry and wet deposition fields (i.e. 2-D spatial patterns and their temporal evolutions).

In the adjoint (i.e. inverse) mode, the model input in the specific case of this study contained measured aerosol concentrations (the so-called sensitivity source function), and the meteorological fields. However, no emissions are used as model input in the adjoint computations. The output (the so-called sensitivity distribution) was a 4-D probability field for the locations of the sources of the observed concentrations. This output specifies the probability that the measured concentration is originated from a specific location or region, it could also be called the footprint of the observations.

In the forward and inverse computations, we used the meteorological fields from the short-term forecasts by the European Centre of Medium-range Weather Forecasts (ECMWF), the fields were extracted every 6 hours. To evaluate the influence of varying meteorological input, the fields of the numerical weather prediction model HIRLAM (the Finnish variant of this model) were also used for a few parallel runs.

The adjoint dispersion computations

The adjoint modelling is a technique to evaluate the footprint of the observations. A ground surface footprint of a single observation is by definition a surface area, which delineates the sources that are responsible for the observed atmospheric concentrations. As a simplification, all sources located within the footprint area would influence this observation, and no sources located outside the footprint area would affect it.

However, the detailed contributions of these sources can be probabilistically evaluated, i.e., the model can be used to evaluate the probability of a specific air parcel to reach the observational site. By integration over all the sources and transport pathways, one can evaluate the spatial and temporal distribution of the probability for the sources to impact a specific measurement. The source areas, for which this probability does not vanish, comprise the footprint that corresponds to this particular observation. Computations of the footprint with standard dispersion models are prohibitively resource-consuming, while the adjoint modelling generates the solution with reasonable efforts (Marchuk 1982, Sofiev *et al*. 2006d).

Assuming the first-order closure of the turbulent diffusion problem with a diagonal eddy diffusivity tensor (so-called *K*-theory closure, *see* Marchuk 1982, Jacobson 1998, Seinfield & Pandis 2006), and linear or linearised chemical reactions (Marchuk 1982), the adjoint dispersion equation can be written in the following form:

$$
\begin{aligned}
& L^{*}\varphi^{*} = S \\
& L^{*} = -\frac{\partial}{\partial t} - \frac{\partial}{\partial x_i}\left(u_i\right) - \frac{\partial}{\partial x_i}\mu_{ii}\frac{\partial}{\partial x_i} + \xi^{*} \\
& \varphi^{*}\left(t = t_{\mathrm{end}}\right) = 0 \\
& \mu_{33}\left.\frac{\partial \varphi^{*}}{\partial x_3}\right|_{x_3 = h_1} = v_d \varphi^{*}\left(h_1\right) \\
& \left.\frac{\partial \varphi^{*}}{\partial x_3}\right|_{x_3 = H} = 0 \\
& \left.\frac{\partial \varphi^{*}}{\partial x_i}\right|_{\left(x_1, x_2\right) \in \partial\Omega} = 0
\end{aligned}
\qquad (1)
$$

where L^{*} is the adjoint dispersion operator that

has been defined in the first row of the equation, φ^* is the sensitivity distribution that arises from the sensitivity source function S, t and x_i are the time and spatial coordinates ($i = 1, 2, 3$), u_i is the ith component of the mean wind, μ_{ii} is the diagonal component for the diffusion coefficient, ξ^* represents the adjoint linear sink term, t_{end} is the end time of the simulations, v_d is the dry deposition velocity at the reference height h_1, and H is the upper boundary of the horizontal computational domain $\partial\Omega$.

For computing the footprint of a single observation in the time series, the specific form of S is calculated as follows:

$$S(x,y,z,t) = \delta(x - x_{st})\delta(y - y_{st})\delta(z - z_{ref}) \times H(t - t_{start})H(t_{end} - t) \quad (2)$$

Here, x_{st} and y_{st} are the coordinates of the station, z_{ref} is the reference height of the monitor inlet, and t_{start}, and t_{end} are the start and end times of the observation, and H is the Heaviside step function [$H(x) = 0$ for $x < 0$ and $H(x) = 1$ for $x \geq 0$]. As a result, the S function is zero everywhere except for the point (x_{st}, y_{st}, z_{ref}) where it is equal to 1 during the observation time. For the footprint of a time series, S should be scaled with actual concentrations measured for every corresponding observation interval.

The adjoint equation is directed backwards in time, so the sensitivity distribution φ^* starts from the receptor with sensitivity S at $t = t_{end}$ and covers the areas where the sources affect the receptor. Importantly, the adjoint formalism is based on linearity assumption regarding all the processes. Since the actual mechanisms are usually nonlinear, various local linearization algorithms have to be applied in order to obtain an analogy to Eq. 1 (for more details *see* Marchuck 1982).

We performed the adjoint simulations separately for each size range. The dry and wet deposition processes are included, however, the simulation setup does not include aerosol dynamics or chemistry. In comparison with the above-outlined footprint dispersion studies published to-date, this setup includes the deposition processes, which may substantially alter the patterns and shorten the predicted footprint areas. The sensitivity source function was constructed based on the aerosol concentrations measured by EAS, with the background concentrations subtracted. The complementary forward simulations included chemical transformation of sulphur oxides after the DMAT model (Sofiev 2000), as well as the deposition processes. However, the aerosol dynamics was not included into the forward simulations either. Being an evident limitation, this did not affect the analysis outcome too strongly because the primary target of the study was the source apportionment of the gaseous precursors rather than the aerosol processes themselves.

Adjoint simulations used mass concentrations rather than number concentration. The relation between these quantities was calculated for each particle size assuming the density of particulate matter to be 1000 kg m^{-3}. The time scale of model runs (a few days) is much longer than the time scale of condensation growth (a few hours) but quite short in comparison with the removal time for fine particles. As a result, for particles in the nucleation and Aitken ranges, the footprint computed refers to the precursors of the aerosol rather than the particles themselves. For coarser particles, especially from the accumulation mode, the obtained footprint reflects the distribution of the direct sources of aerosols.

The forward dispersion computations

Forward model runs were performed in order to investigate the contribution of anthropogenic and natural emissions to the observed concentrations. The emission data of these runs include (i) primary particulate matter (PM_{10}), (ii) primary fine particlulate matter ($PM_{2.5}$), (iii) sulphur dioxide, (iv) sulphate and (v) sea salt. Emissions of primary particulate matter, sulphur dioxide and sulphate were gathered from EMEP database for Europe, excluding the most southern and western parts, as those regions do not have any substantial influence on the concentrations in the considered boreal region. A more detailed database of sources was applied for Finland. The Finnish emission inventory has a 1-km resolution for area sources and includes about 250 point sources. The main aerosol components that were not included in the modelling are nitrates

and ammonium. Seasonal, weekly and diurnal variations followed Sofiev *et al*. (1996). The emissions of sea salt are embedded in SILAM and governed by wind speed and sea water salinity by using the updated paramaterisation of Monahan *et al*. (1986) modified with data of Mårtensson *et al*. (2003).

SILAM model computes the conversion of SO_2 to sulphate via a single-reaction transformation scheme (Sofiev 2000). No other chemical reactions were included, chemical components of primary particles and sea salt were regarded as passive tracers.

The horizontal resolution of model output was 20 km, and the concentration and sensitivity distribution fields were saved once in every 15 minutes. Output in the vertical direction consisted of five layers up to the height of 3150 m above the ground surface. For the numerical results presented here, the output fields were averaged over the two lowest layers (from the ground level up to a height of 150 m). The wind vectors overlaid in the concentration maps were also averaged over the two lowest layers, corresponding to a layer from the ground level to approximately a height of 150 m.

Results

The selection of the episodic events

The classification of aerosol events in this study is based on four size ranges listed in Table 1. Events are classified qualitatively (*see* Fig. 2), assuming each peak is significantly exceeding the stated background level in corresponding size range to be an event. We expect that behind each of these events (peaks) should be a particle formation, evolution or transport process (or coincidence of processes) that is not common during the entire measurement campaign. In following we examine the possible processes.

During the analysis, we paid special attention to the conditions that promote or prohibit the nucleation events. Although the precise mechanism and all conditions for the nucleation burst are not known, a low concentration of coarse aerosol particles (i.e. a low condensation sink) is typically necessary (Kulmala *et al*. 2005). Nucleation events therefore occur predominantly during dry and sunny weather with clean air masses and sufficient solar radiation. Due to biogenic emissions of precursors, the boreal forest is an important source of secondary fine aerosols (Tunved *et al*. 2006) produced via oxidation of isoprene and monoterpenes (Kavouras *et al*. 1998, Kourchev *et al*. 2005, 2008). It has been found that nucleation events in boreal forests occur even in late winter with snow cover present, due to life activities in evergreen tree crowns during sufficient solar radiation (Kulmala *et al*. 2001, 2004d).

Another natural source of particles is the sea. Apart from micrometer-size particles, 10-nm size particles were registered over the sea but their origin had not been completely clear (Covert *et al*. 1992, Mårtensson *et al*. 2003, Clarke *et al*. 2006). Finally, a well-known but totally different environment for the formation of nanometer particles is the urban photochemical smog (McMurry and Eisele 2005).

The measured mass concentrations of the four considered aerosol size ranges contain three nucleation events (sudden appearing and following growth of a large number of nanometer-size particles), three high-concentration episodes of coarse and accumulation particles and one episode, where concentrations of all particles except nucleation range (i.e. Aitken, accumulation and coarse) were elevated (Fig. 2). The nucleation-size aerosol peaks occurred on 30 April (event 1), and on 5 and 9 May (events 2 and 3, respectively). The nucleation bursts occurred during the low background concentration of pre-existing (accumulation and coarse mode) aerosol particles.

We selected two categories of episodes for a detailed examination: (i) periods with the highest measured concentrations of nucleation aerosol, and (ii) for contrast, other specific episodes, and their footprints are compared. In particular, we address the three detected nucleation events and three events of simultaneous highest concentration of coarse and accumulation particles, referred henceforward as accumulation and coarse peaks or A & C peaks. Although these two size ranges are of different physical origin, they often occur simultaneously in industrial and urban emissions.

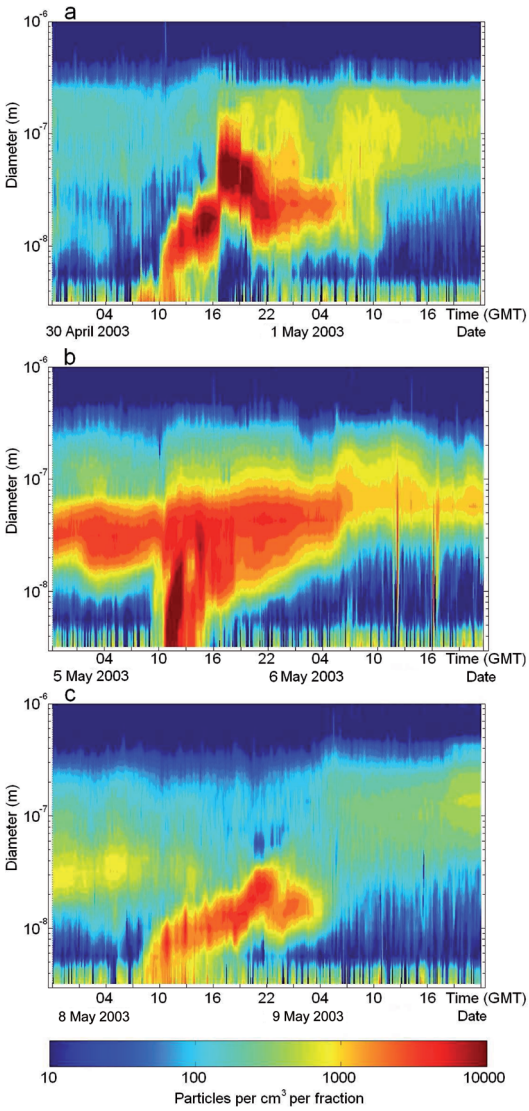

Fig. 3. Time-size concentrations of nucleation events: (**a**) event 1 (30 April–1 May), (**b**) events 2 (5–6 May) and 3 (8–9 May).

Nucleation events

During the LAPBIAT measurement campaign at Värriö three nucleation events were observed (Fig. 3).

First nucleation event

This event occurred on 30 April 2003. It can be characterized as an interrupted nucleation event. Before event 1, concentrations in all size modes were anomalously low and, after a few hours, a highly polluted air mass was observed with large amounts of particles of Aitken, accumulation and coarse modes (Ruuskanen *et al.* 2007). A remarkable amount of nucleation particles appeared again a few hours later, after the exchange of the air masses.

The inverse model run (Fig. 4a) shows that the most probable source areas of nucleation aerosol during the first event are located to the east of Värriö. During the preceding night, the air masses were transported through the Norwegian–Russian border in the vicinity of the Nikel metallurgy industry, but they were not transported over any intensive source areas. Corresponding forward simulations show that there was practically no sulphate in the air around Värriö at the beginning of the event (Fig. 4b). An excessive concentration of sulphate arrived from Kola Peninsula only during the next six hours (Figs. 4c and 5).

The observation of the nucleation event (rise of the concentration of nucleation aerosol) was interrupted by arriving polluted plume (about 16:00) that contained sulphates and anthropogenic particles (*see* Figs. 3a and 5). The total modelled PM (Fig. 4) also includes sea salt from the northern sea areas and the Baltic Sea, but their fraction was small. The modelled total of primary PM and sulphate in the polluted plume was about 8 μg m^{-3} including about 5 μg m^{-3} of sulphates, which is in fair agreement with the PM_{10} estimated from EAS measurements (about 10 μg m^{-3}).

Second nucleation event

This nucleation event started on 5 May at 11:00 GMT, then a large number of nanometer-size particles grew to Aitken sizes in late evening. This is a typical strong nucleation event with relatively high growth rate around 4 nm h^{-1}. Inverse model computations show that the air masses were transported during the two previous days over the continental areas of northern Sweden and central Finland, and were also transported over the Gulf of Bothnia (Fig. 6).

When the nucleation event began at Värriö, a

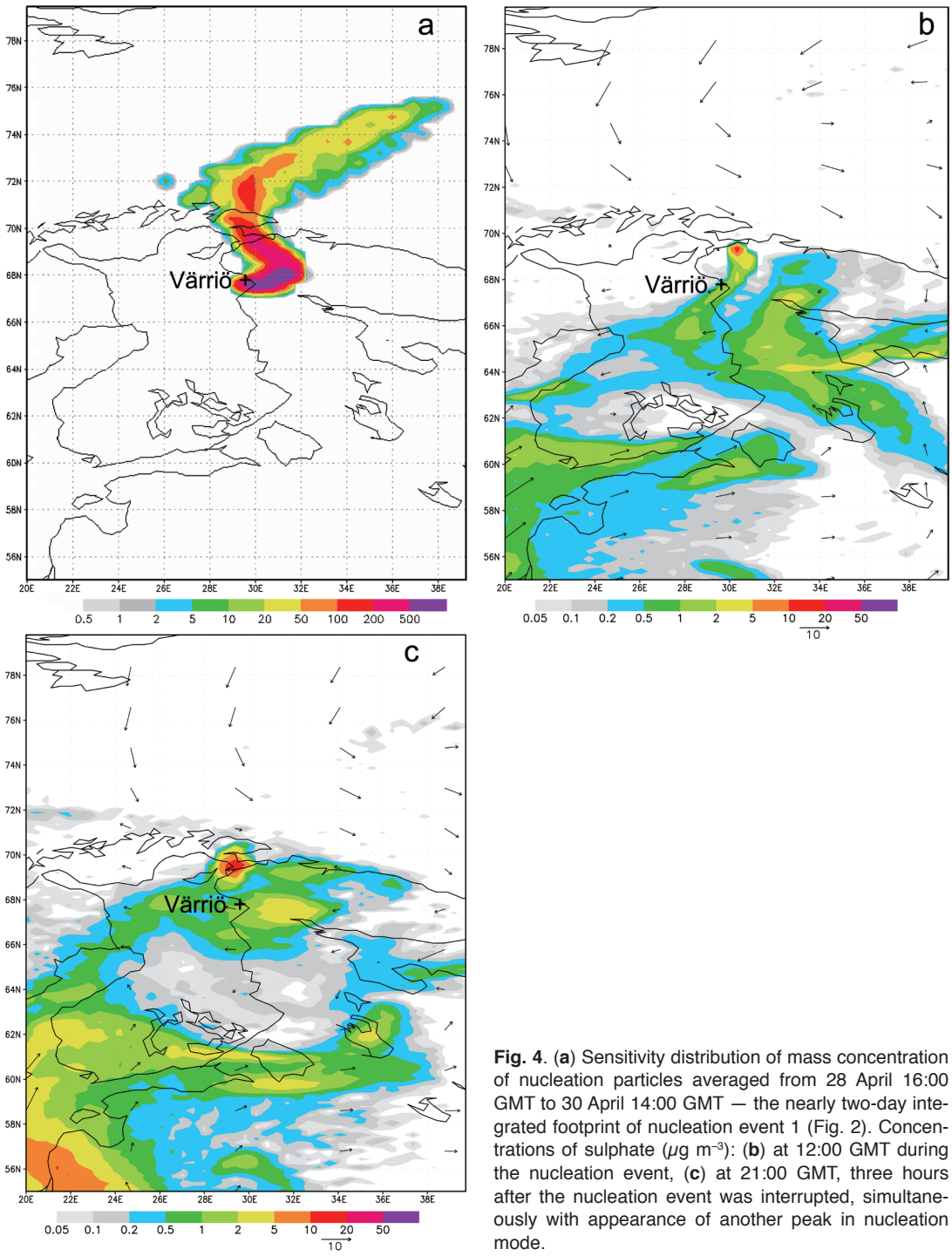

Fig. 4. (**a**) Sensitivity distribution of mass concentration of nucleation particles averaged from 28 April 16:00 GMT to 30 April 14:00 GMT — the nearly two-day integrated footprint of nucleation event 1 (Fig. 2). Concentrations of sulphate (μg m^{-3}): (**b**) at 12:00 GMT during the nucleation event, (**c**) at 21:00 GMT, three hours after the nucleation event was interrupted, simultaneously with appearance of another peak in nucleation mode.

well-defined footprint was formed that extended over the Finnish Lapland from north-east to south-west (Fig. 6b). During and shortly after this nucleation event the forward model computations did not show any advection of substantial concentrations of sulphate over Värriö. Only on 6 May, was there some slight influence of sulphate pollution from central Europe.

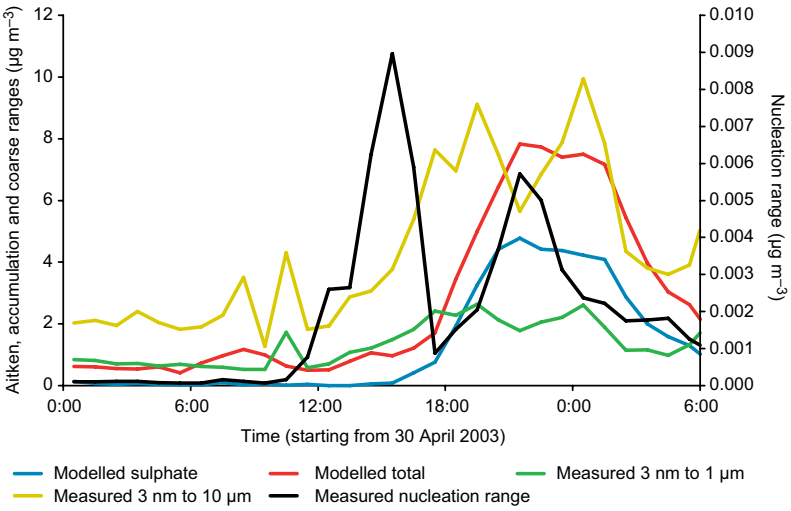

Fig. 5. Measured concentrations of aerosol in nucleation size range and in two other size classes (these are approximately equal to the PM_1 and PM_{10}), and modelled $PM_{2.5}$ concentrations that include sulphate, sea salt and primary $PM_{2.5}$, during formation and break-up of nucleation event 1.

The nucleation event number 2 on 5 May (Fig. 6) was followed by relatively high concentrations of Aitken nuclei during the following couple of days (cf. Fig. 2a). When the event started, the source area of Aitken nuclei extended along the western coast of Finland to the Baltic Sea and reached the coast of Latvia (Fig. 7). The maximum of Aitken size range particle concentration at Värriö occurred a few hours later than that of the nucleation particles. Remarkable concentrations of Aitken nuclei were observed between the late evening of 5 May and the evening of 6 May. Thus, we suppose that these Aitken nuclei were the aged particles from the nucleation event that took place during 5 May all over the western Finland and was observed at Värriö as two sequential peaks of concentrations — first of the nucleation-sized particles and then of Aitken ones.

Third nucleation event

In the case of nucleation event on 8 May (Fig. 8), the air masses were transported from the Norwegian Sea. A well-defined footprint was formed that extended over the Finnish and Norwegian Lapland from north-west to south-east (Fig. 8b). This event can be described as a typical nucleation event in Finnish Lapland (Vehkamäki *et al.* 2004).

Description of Aitken, accumulation and coarse particle events

Contrary to simulations of the footprints of nucleation particles, the model tracing of larger-size aerosol fractions indicated the influence of anthropogenic activities. The concentration of accumulation particles was used as the main indicator of pollution from remote sources due to its longest lifetime in the atmosphere.

Permanently high aerosol concentrations bewteen 28 and 29 April were influenced by large areas of north-western Russia and Baltic states (Fig. 9). Then the footprint of the observation shifted to the north and to the east and finally reached the observation site being also enriched with emissions from Kola Peninsula.

The highest mass concentrations of particles, about 30 μg m^{-3}, were observed in the late evening of 2 May (Fig. 2). The inverse model run suggests that the origin of particles was located at the westernmost areas of Kola (Fig. 9a). The forward run is based on the EMEP database with the corrected location of the Nikel smelter (for details regarding corrected location *see* Kaasik *et al.* 2007) (Fig. 10).

Although the plume from Nikel is obviously the reason of the peak of coarse (and also accumulation size range) particles, the SILAM model with ECMWF meteorological data failed to predict that peak in quantitative terms: the monitor-

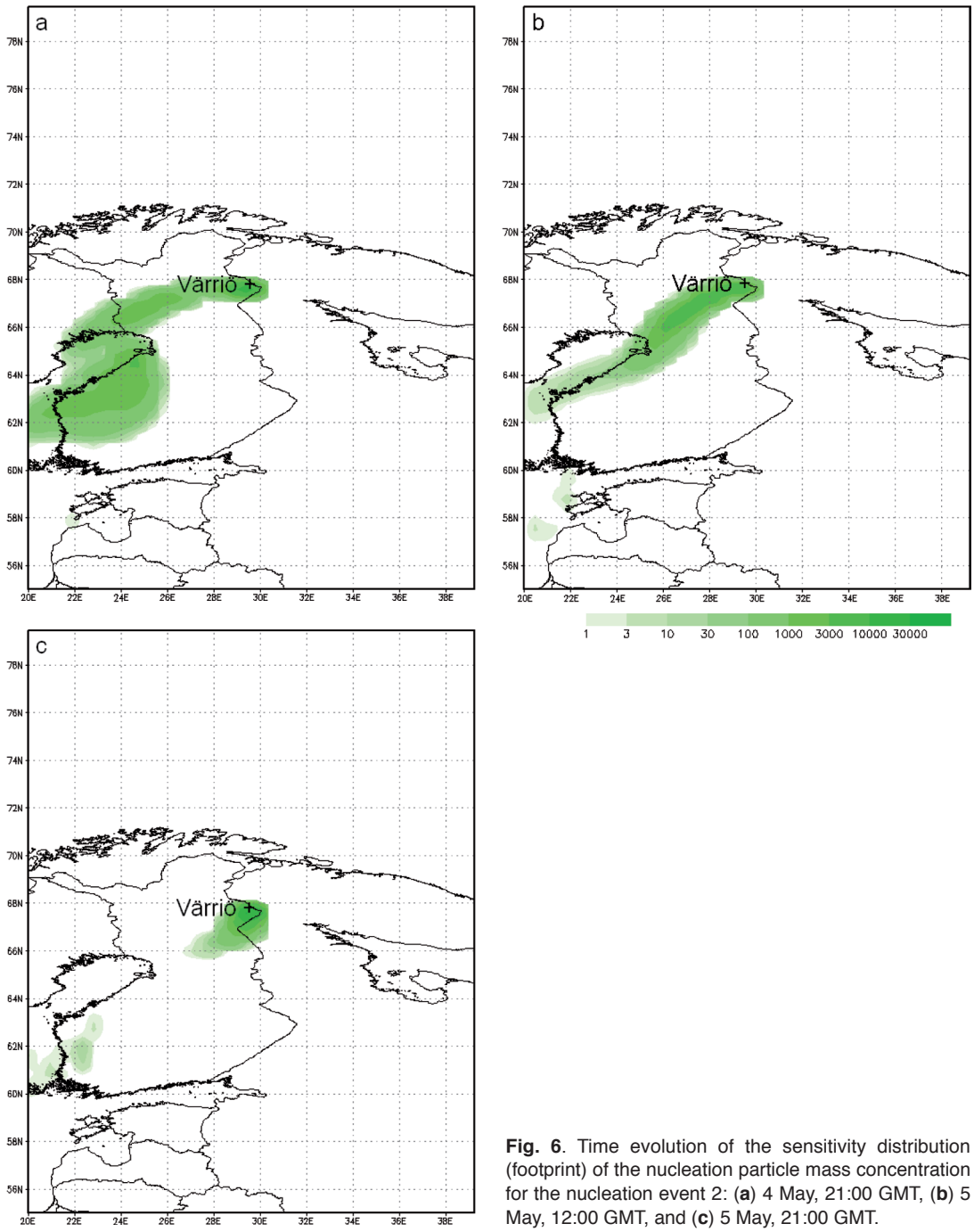

Fig. 6. Time evolution of the sensitivity distribution (footprint) of the nucleation particle mass concentration for the nucleation event 2: (**a**) 4 May, 21:00 GMT, (**b**) 5 May, 12:00 GMT, and (**c**) 5 May, 21:00 GMT.

ing station remains just at the edge of the narrow plume, 20–30 km west from its axis. Thus, there is only a very small increase from background level in concentrations predicted for Värriö. To clarify the impact of meteorological input to the results, a parallel model run was performed with short-term forecast from the HIRLAM model (the variant of this model developed at the Finn-

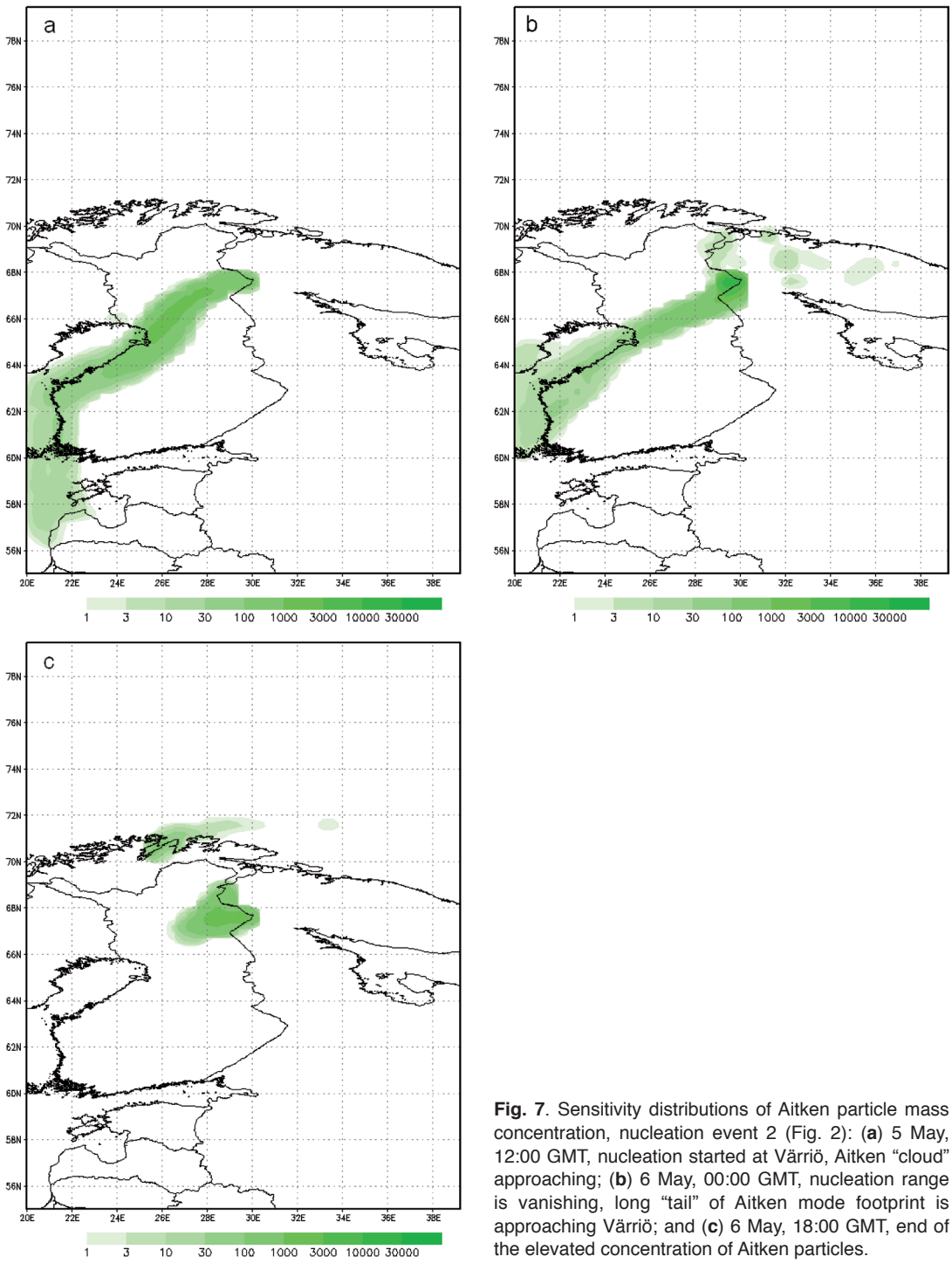

Fig. 7. Sensitivity distributions of Aitken particle mass concentration, nucleation event 2 (Fig. 2): (**a**) 5 May, 12:00 GMT, nucleation started at Värriö, Aitken "cloud" approaching; (**b**) 6 May, 00:00 GMT, nucleation range is vanishing, long "tail" of Aitken mode footprint is approaching Värriö; and (**c**) 6 May, 18:00 GMT, end of the elevated concentration of Aitken particles.

ish Meteorological Institute).

The results look qualitatively similar (Fig. 11), but the plume from the Nikel industrial complex computed using the HIRLAM meteorological fields was transported first to south-southwest and then eastwards exactly over Värriö, this

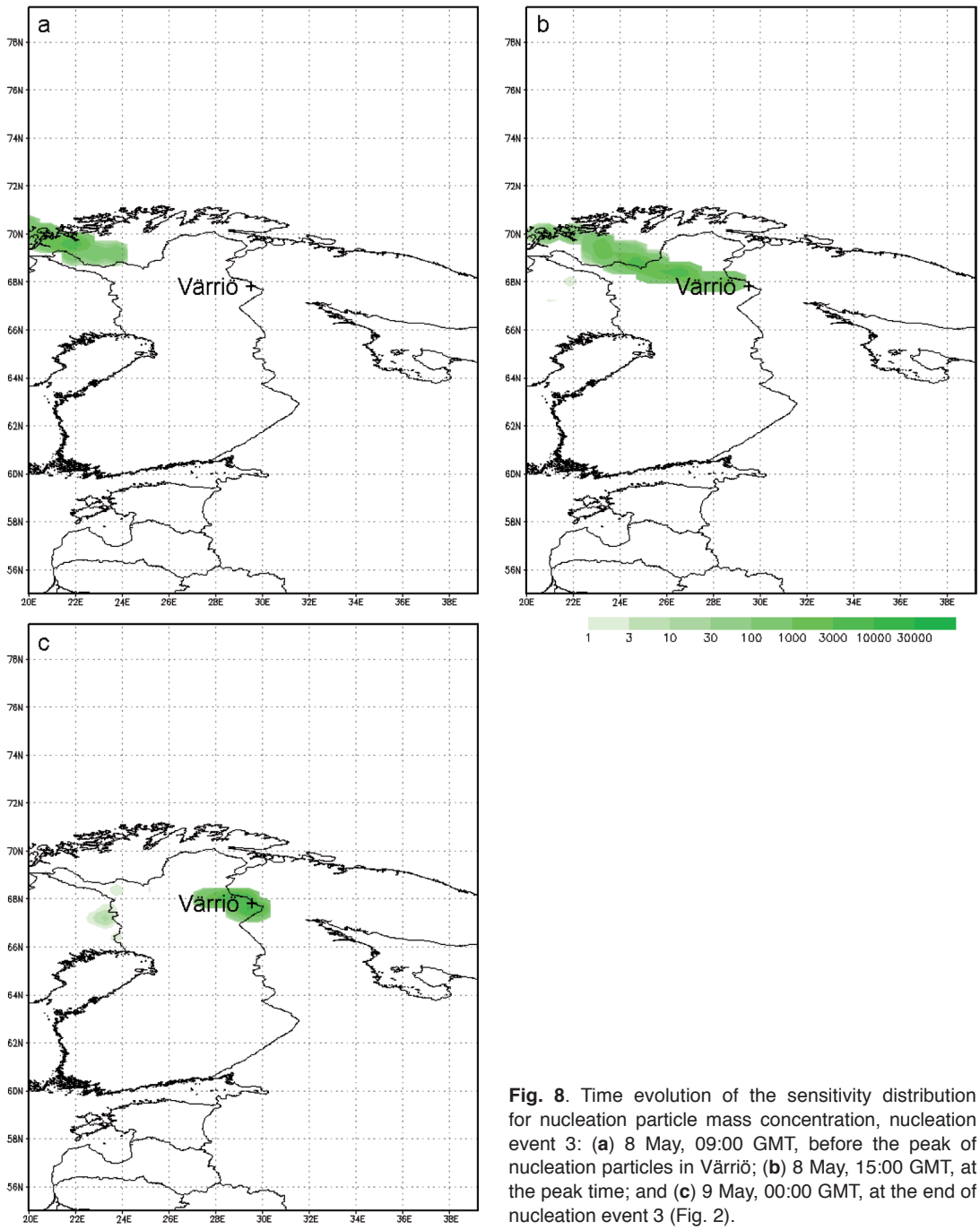

Fig. 8. Time evolution of the sensitivity distribution for nucleation particle mass concentration, nucleation event 3: (**a**) 8 May, 09:00 GMT, before the peak of nucleation particles in Värriö; (**b**) 8 May, 15:00 GMT, at the peak time; and (**c**) 9 May, 00:00 GMT, at the end of nucleation event 3 (Fig. 2).

resulted in a better agreement of model predictions with the observed values (Fig. 12).

The model computations using the ECMWF and HIRLAM data failed to predict the exact position and size of aerosol peaks on 28 and 29 April (Fig. 12b).

Discussion

Three particle formation events (30 April, 5 May and 8 May) were selected for a more detailed analysis. The most informative with respect to the aerosol formation mechanisms was the second

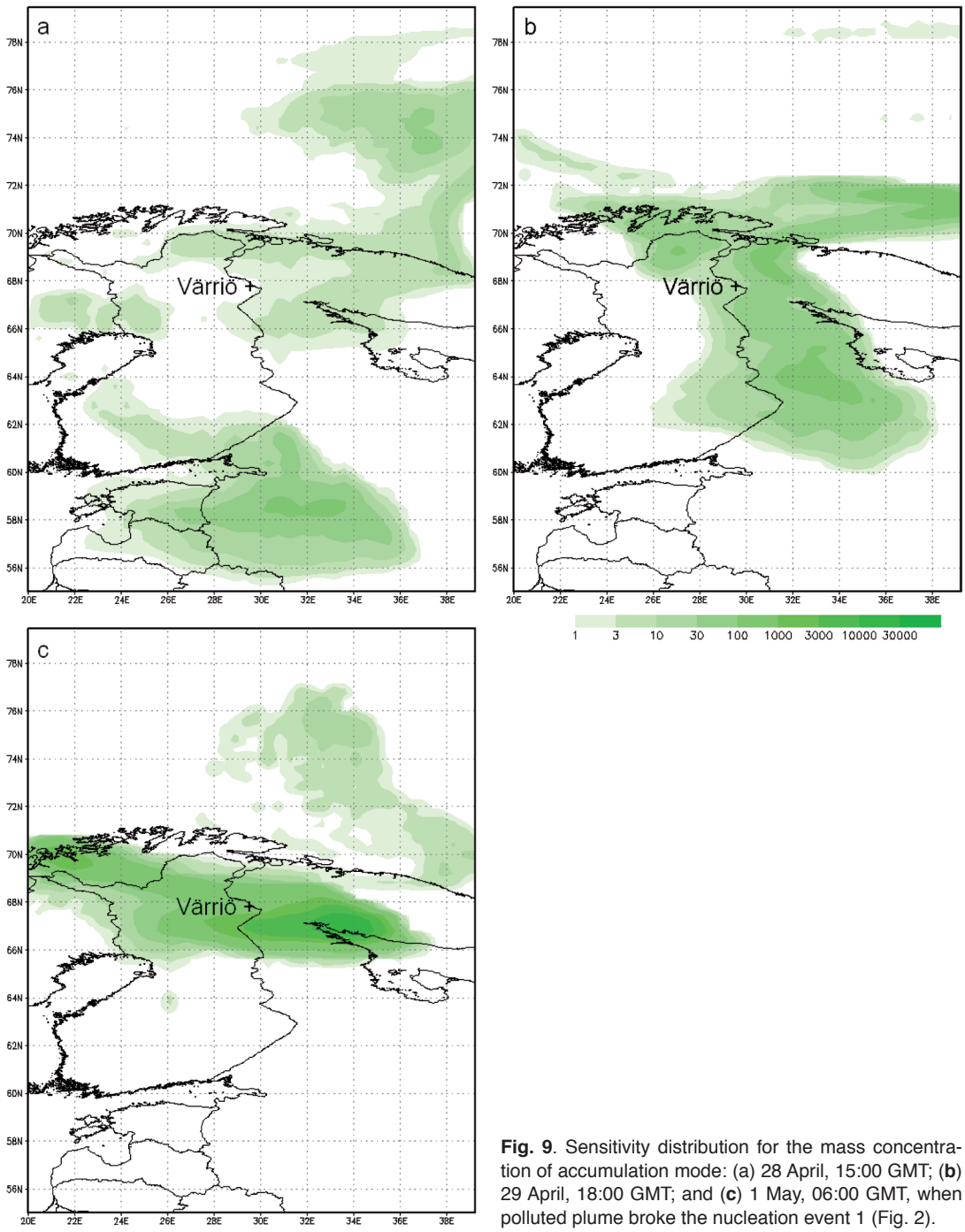

Fig. 9. Sensitivity distribution for the mass concentration of accumulation mode: (a) 28 April, 15:00 GMT; (**b**) 29 April, 18:00 GMT; and (**c**) 1 May, 06:00 GMT, when polluted plume broke the nucleation event 1 (Fig. 2).

one, as it was intensive enough and not disturbed by arrival of polluted plumes. Prior to the episode, the air masses spent more than two days over the forested areas with scarce human activities and no major influence of industrial pollution.

Hence, the main mechanism triggering the growth of particles in this case was most likely the condensation of biogenic volatile hydrocarbons that had been accumulated in the air during previous days (for details of the mechanism,

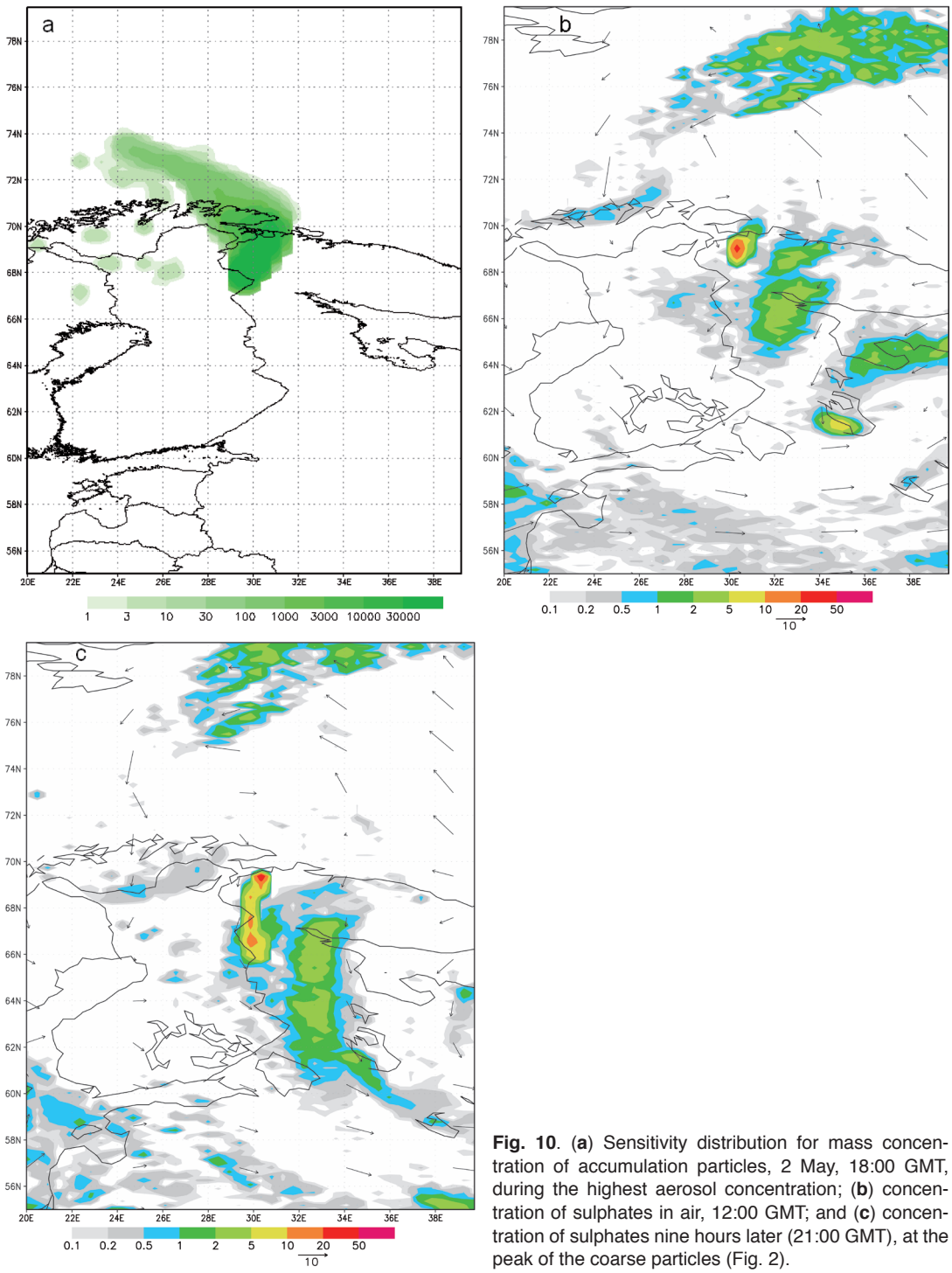

Fig. 10. (**a**) Sensitivity distribution for mass concentration of accumulation particles, 2 May, 18:00 GMT, during the highest aerosol concentration; (**b**) concentration of sulphates in air, 12:00 GMT; and (**c**) concentration of sulphates nine hours later (21:00 GMT), at the peak of the coarse particles (Fig. 2).

see Kulmala *et al*. 2004b, 2004c, Tunved *et al*. 2006). Taking into account the footprints of both nucleation and aged Aitken particles, we can estimate that the area of gathering the precursors may have extended for approximately 1000 kilometres from south-west to north and north-east.

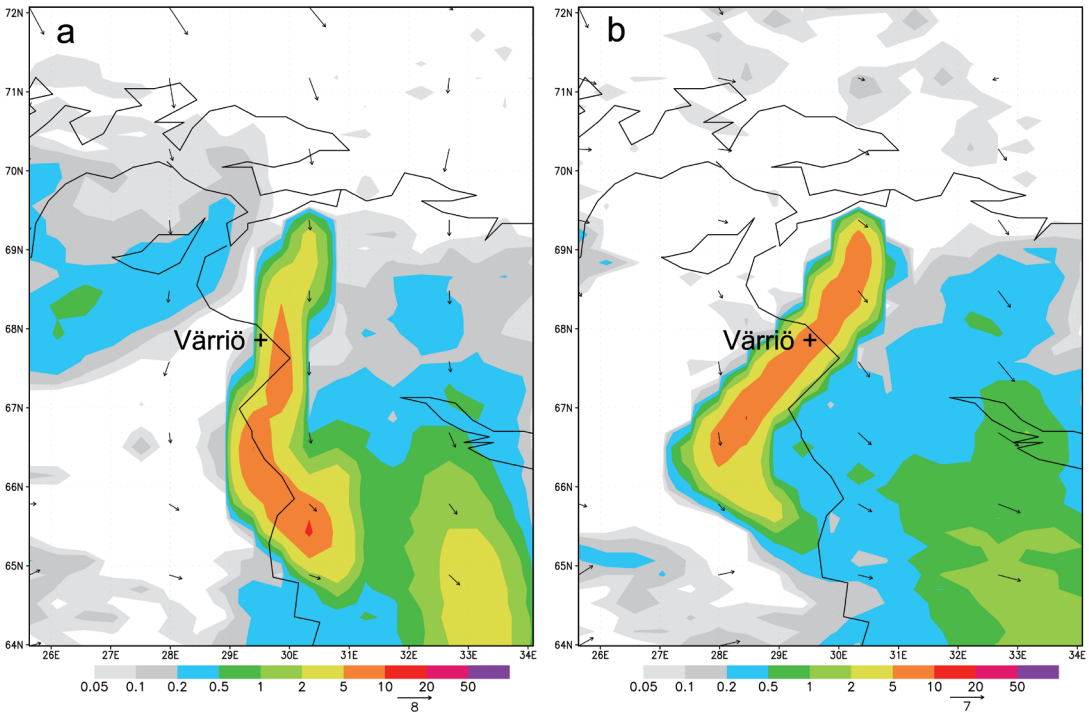

Fig. 11. Modelled concentrations of sulphate (μg m^{-3}) at the top of coarse aerosol peak 3 (3 May, 00:00 GMT): (**a**) applying ECMWF meteorological fields, (**b**) applying HIRLAM meteorological fields.

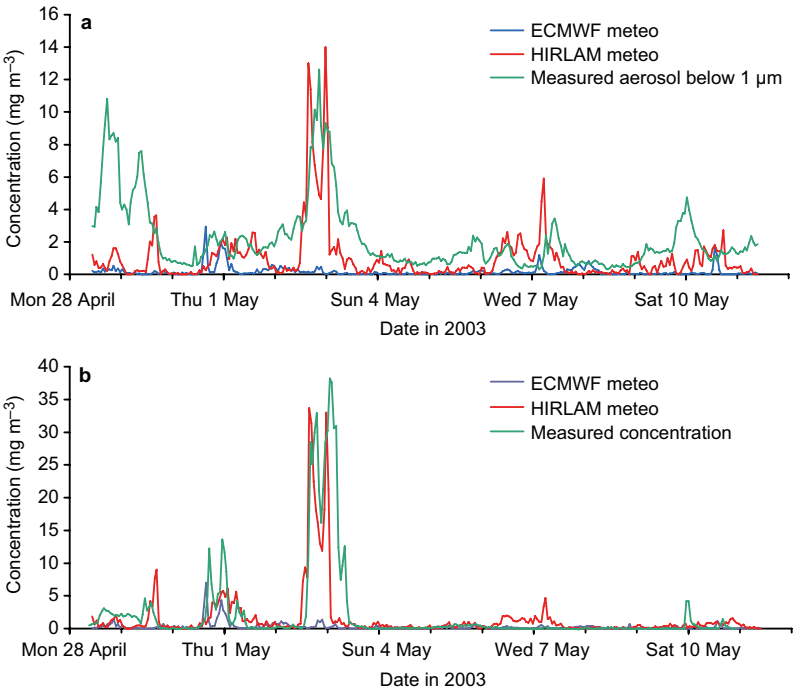

Fig. 12. Comparison of measured concentrations with model predictions, applying different meteorological data: (**a**) sulphate ion, and (**b**) sulphur dioxide.

However, as the air masses were transported over the Baltic Sea, we cannot exclude the influence of marine emissions.

The first nucleation event is interesting due to the sharp change of air masses at Värriö that interrupted its observation. It was also a more complicated case for the analysis as compared with the second event. The first part of the episode followed the typical pattern. During that time, the emissions from the Arctic Ocean or biogenic emissions from forests in Lapland could have affected the composition of the plume shortly before it reached the measurement site. The area considered was still covered with snow and the temperatures were slightly below zero, but solar heating of tree crowns could induce some vegetation activity. As the air masses were advected very close to the Nikel metallurgy factory, one cannot exclude some influence of gaseous emissions from its surrounding infrastructure as well.

Regarding the interruption of the first nucleation event observations at the station, the forward model run reproduced the time of arrival of sulphate-rich air from Nikel plant with accuracy close to the 15-minute model time step (about 16:00–17:00 GMT, 30 April). The concentrations of sulphates were nearly the same as the measured fine-aerosol level at that time (2–5 μg m^{-3}). This indicates that the measured rapid increase of aerosol mass concentration occurred due to industrial pollution from the Nikel metallurgical complex.

The source apportionment of the last particle formation event (nucleation event 3 on 8 May) is straightforward: the air was advected during less than 10 hours from the Norwegian Sea over northern Lapland. According to this time scale, most of the particle growth occurred over the continental areas, but it can start at the sea coastline and marine emissions might take part in triggering the formation of particles.

High levels of particles during 28–29 April occurred probably due to diffuse emissions from North-western Russia and Baltic states, in contrary to the above peaks during 30 April–3 May (Fig. 9) that originated from metallurgical industries of Kola Peninsula (Russia). Lower concentrations than in the later events but still remarkable levels of SO_2 suggest considerable age of the plume and impact of remote anthropogenic sources, such urban emissions in the St. Petersburg area pointed by the adjoint run of SILAM. The missing part of modelled PM could then consist of nitrates, ammonia, dust, etc.

It is also possible that the first peak of coarse and accumulation modes in the evening of 28 April might include an influence of a local sauna at Värriö biological station, about 2 km southwest of the monitoring site: wind was blowing from southern directions and complex landscape favoured an efficient dispersion of emissions. A low SO_2 concentration is also more typical for wood burning than for industry. However, the model resolution was insufficient to detect such a small-scale effect. The probable origins of all events are presented in Table 2.

Both forward and adjoint simulations were performed with two input meteorological datasets in order to assess (at a qualitative level) the uncertainties caused by the usage of particular meteorological datasets for the disper-

Table 2. Identified origins of peaks presented in Fig. 2.

Event	Dates	Identified area of origin	Probable source
Accumulation and coarse peak 1	28 April	St. Petersburg and surroundings, surroundings of Värriö	urban and industrial emissions, local saunas
Accumulation and coarse peak 2	29 April	St. Petersburg and surroundings	urban and industrial emissions
Nucleation 1	30 April	Regions mainly in Russia and Norway, to the east and to the north of Värriö	emissions from forests, possible some industrial influence
Aitken particle event	30 April–1 May	Kola peninsula, Russia	industrial emissions
Accumulation coarse peak 3	2–3 May	Kola peninsula, Russia	industrial emissions
Nucleation 2	5 May	Southern Lapland	emissions from forests
Nucleation 3	8 May	Arctic Sea, northern Lapland	possible marine emissions

sion modelling. Such uncertainties can be very large from the point of view of a single-station observation (*see* Figs. 11 and 12). In particular, the concentrations predicted for the specific site can differ by orders of magnitude depending on meteorological input. This sensitivity, however, is to be expected because the pollution pattern over the region is almost entirely dictated by few strong almost-point sources. As a result, even a small uncertainty in positioning of the plumes from these sources can lead to large differences in absolute concentrations registered at a single monitoring site. This holds for both forward and adjoint dispersion analysis.

In general, the plumes calculated with the HIRLAM meteorological data were narrower and the pollutant concentrations at the ground level were higher than in the corresponding plumes computed using the fields of the ECMWF model. These findings qualitatively corroborate the previous results of Sofiev *et al.* (2006c), who compared the outcomes of the SILAM model simulations with the ETEX data, using two HIRLAM model versions and the ECMWF model. In the current case, during the third peak of coarse particles concentrations, the surface-level wind directions modelled by ECMWF and HIRLAM differ for up to 30° (Fig. 11). Thus, the computations using the ECMWF wind fields suggested that the plume from the Nikel plant was transported directly to the south, while the corresponding computations using the HIRLAM data resulted in a more complicated pattern of concentrations.

The simulations were performed without explicit treatment of aerosol dynamics while the chemical transformations were taken into account only in the forward mode. These evident limitations, however, do not affect the outcome of the analysis because the main goal of the study was to evaluate the sources of aerosol precursors and qualitatively evaluate the conditions favouring the nucleation events. Simulation of the events themselves was outside the scope of the study. The simplified model configuration significantly reduced the resources needed for the computations and allowed, in particular, the ensemble-type uncertainty analysis of the dispersion paths of the air masses before and during the nucleation events.

Conclusions

Adjoint dispersion modelling can be used as an assessment tool for prediction of the observational footprint at regional scale. Particularly, it localises the areas contributing to the concentrations of both aerosol particles and their precursors, and provides a detailed time schedule of a new particle formation event in the plume, while it is transported towards the station.

Combination of adjoint and forward modelling of transport of species from known sources makes it possible to distinguish more accurately between the local and non-local sources. A cross-checking of the results based on inverse and forward computations is also useful for the quality assurance of models.

According to the size of the computed footprints, the nucleation and particle-growth events could possibly extend over hundreds and sometimes thousands of kilometres (*see* Vana *et al.* 2004). The regional scale of the events may partly explain their complicated appearance in the observations. The chemical and physical properties of the air masses may change substantially during the atmospheric transport, due to deposition (in particular, scavenging), the varying anthropogenic and natural emissions, and the physical and chemical transformation processes.

Application of ensemble-type approaches with several input datasets can be of importance for both forward and inverse tasks, in particular, when the corresponding sources are geographically limited and result in fairly narrow plumes. Thus, in one of the analysed episodes, there was a remarkable difference between the results computed with the meteorological fields of the ECMWF and HIRLAM models.

The SMEAR I station is a convenient test site for mesoscale air quality model applications, due to the absence of significant local sources of air pollution in close neighbourhood (on the scale of tens of kilometres), an extensive sector for wind directions from pristine regions, and a presence of a few well-identified intensive point sources at the distances of 100–200 kilometres.

Acknowledgements: Basic modelling activities with SILAM were funded by the Nordic Research Board (NordForsk), young researcher mobility scholarship no. 50081 (for

Marko Kaasik), Estonian Science Foundation, grants 7005 and 8342 and Estonian National Targeted Financing Project SF0180038s08. The SILAM model development was supported by the EU-GEMS and ESA-PROMOTE projects. This study was a part of the COST actions 728 and ES0602.

References

Barletta B., Meinardi S., Simpson I.J., Atlas E.L., Beyersdorf A.J., Baker A.K., Blake N.J., Yang M., Midyett J.R., Novak B.J., McKeachie R.J., Fuelberg H.E., Sachse G.W., Avery M.A., Campos T., Weinheimer A.J., Rowland, F.S. & Blake D.R. 2009. Characterization of volatile organic compounds (VOCs) in Asian and north American pollution plumes during INTEX-B: identification of specific Chinese air mass tracers. *Atmos. Chem. Phys.* 9: 5371–5388.

Bergamaschi P., Krol M., Dentener F., Vermeulen A., Meinhardt F., Graul R., Ramonet M., Peters W. & Dlugokencky E.G. 2005. Inverse modelling of national and European CH_4 emissions using the atmospheric zoom model TM5. *Atmos. Chem. Phys.* 5: 2431–2460.

Clarke A., Owens S. & Zhou J. 2006. An ultrafine sea-salt flux from breaking waves: Implications for cloud condensation nuclei in the remote marine atmosphere. *J. Geophys. Res.* 111, D06202, doi:10.1029/2005JD006565.

Covert D.S., Kapustin V.N., Quinn P.K. & Bates T.S. 1992. New particle formation in the marine boundary layer. *J. Geophys Res.* 97: 20581–20589.

Draxler R.R. & Rolph G.D. 2003. *HYSPLIT (HYbrid Single-Particle Lagrangian Integrated Trajectory) model*. NOAA Air Resources Laboratory, Silver Spring, MD, also available at http://www.arl.noaa.gov/ready/hysplit4.html.

Elbern H. & Schmidt H. 1999. A four dimensional variational chemistry data assimilation schmeme for eulerian chemistry transport modeling. *J. Geophys. Res.* 104: 18583–18598.

Elbern H., Schmidt H. & Ebel A. 1997. Lagrangian four-dimensional variational data assimilation of chemical species. *J. Geophys. Res.* 102: 15967–15985.

Elbern H., Strunk A., Schmidt H. & Talagrand O. 2007. Emission rate and chemical state estimation by 4-dimensional variational inversion. *Atmos. Chem. Phys.* 7: 3749–3769.

Fisher M. & Lary J. 1995. Lagrangian four-dimensional variational data assimilation of chemical species. *Q. J. R. Meteorol. Soc.* 121: 1681–1704.

Hari P., Kulmala M., Pohja T., Lahti T., Siivola E., Palva L., Aalto P., Hämeri K., Vesala T., Luoma S. & Pulliainen E. 1994. Air pollution in eastern Lapland: challenge for an environmental measurement station. *Silva Fennica* 28: 29–39.

Heo J.-B., Hopke P.K. & Yi S.-M. 2009. Source apportionment of $PM_{2.5}$ in Seoul, Korea. *Atmos. Chem. Phys.* 9: 4957–4971.

Jacobson M. 1998. *Fundamentals of atmospheric modelling*. Cambridge University Press, Cambridge.

Kaasik M., Prank M., Sofiev M. & Kukkonen J. 2007. Atmospheric transport model SILAM applied in Estonia. In: Vainio J., Pomoell J. & Luhivuori M. (eds.), *Proceedings of the XLI Annual Conference of the Finnish Physical Society*. Report Series in Physics HU-P-267, Department of Physical Sciences, University of Helsinki.

Kaasik M., Prank M., Kukkonen J. & Sofiev M. 2008. A suggested correction to the EMEP database regarding the location of major industrial air pollution source in Kola Peninsula. In Borrego C. & Miranda A.I. (eds.), *Air Pollution Modeling and Its Application XIX*, NATO Science for Peace and Security Series C, Environmental Security, Springer, Dordrecht, pp. 331–338.

Kalnay E. 2003. *Atmospheric modeling, data assimilation and predictability*. Cambridge University Press, Cambridge.

Kavouras I.G., Mihalopoulos N. & Stephanou E.G. 1998. Formation of atmospheric particles from organic acids produced by forests. *Nature* 395: 683–686.

Kourchev I., Ruuskanen T., Maenhaut W., Kulmala M. & Claeys M. 2005. Observation of 2-methyltetrols and related photo-oxidation products of isoprene in boreal forest aerosols from Hyytiälä, Finland. *Atmos. Chem. Phys.* 5: 2761–2770.

Kourchev I., Ruuskanen T., Keronen P., Sogacheva L., Dal Maso M., Reissell A., Xhi X., Vermeylen R., Kulmala M., Maenhaut W. & Claeys M. 2008. Determination of isoprene and α/β-pinene oxidation products in boreal forest aerosols from Hyytiälä, Finland: diurnal variations and possible link with particle formation events. *Plant Biology* 10: 138–149.

Kulmala M., Kerminen V.-M. & Laaksonen A. 1995. Simulations on the effect of sulphuric acid formation on atmospheric aerosol concentrations. *Atmos. Environ.* 29: 377–382.

Kulmala M., Petäjä T., Mönkkönen P., Koponen I.K., Dal Maso M., Aalto P.P., Lehtinen K.E.J. & Kerminen V.-M. 2005. On the growth of nucleation mode particles: source rates of condensable vapour in polluted and clean environments. *Atmos. Chem. Phys.* 5: 409–416.

Kulmala M., Vehkamäki H., Petäjä T., Dal Maso M., Lauri A., Kerminen V.-M., Birmili W. & McMurry P.H. 2004a. Formation and growth rates of ultrafine atmospheric particles: a review of observations. *J. Aerosol Sci.* 35: 143–176.

Kulmala M., Laakso L., Lehtinen K.E.J., Riipinen I., Dal Maso M., Anttila T., Kerminen V.-M., Hõrrak U., Vana M. & Tammet H. 2004b. Initial steps of aerosol growth. *Atmos. Chem. Phys.* 4: 2553–2560.

Kulmala M., Suni T., Lehtinen K.E.J., Dal Maso M., Boy M., Reissell A., Rannik Ü., Aalto P., Keronen P., Hakola H., Bäck J., Hoffmann T., Vesala T. & Hari P. 2004c. A new feedback mechanism linking forests, aerosols, and climate. *Atmos. Chem. Phys.* 4: 557–562.

Kulmala M., Hämeri K., Aalto P.P., Mäkela J.M., Pirjola L., Nilsson E.D., Buzorius G., Rannik Ü., Dal Maso M., Seidl W., Hoffman T., Janson R., Hansson H.-C., Viisanen Y., Laaksonen A. & O'Dowd C.D. 2001. Overview of the international project on biogenic aerosol formation in the boreal forest (BIOFOR). *Tellus* 53B:

324–343.

Kulmala M., Rannik Ü., Pirjola L., Dal Maso M., Karimäki J., Asmi A., Jäppinen A., Karhu V., Korhonen H., Malvikko S.-P., Raittila J., Romakkaniemi S., Suni T., Yli-Koivisto S., Paatero J., Hari P. & Vesala T. 2000. Characterization of atmospheric trace gas and aerosol concentrations at forest sites in southern and northern Finland using back trajectories. *Boreal Env. Res.* 5: 315–336.

Kulmala M., Kerminen V.-M., Laaksonen A., Riipinen I., Sipilä M., Ruuskanen T. M., Sogacheva L., Hari P., Bäck J., Lehtinen K.E.J., Viisanen Y., Bilde M., Svenningsson B., Lazaridis M., Tørseth K., Tunved P., Nilsson E. D., Pryor S., Sørensen L.-L., Hõrrak U., Winkler P.M., Swietlicki E., Riekkola M.-L., Krejci R., Hoyle C., Hov Ø., Myhre G. & Hansson H.-C. 2008. Overview of the biosphere–aerosol–cloud–climate interactions (BACCI) studies. *Tellus* 60B: 300–317.

Kulmala M., Boy M., Suni T., Gaman A., Raivonen M., Aaltonen V., Adler H., Anttila T., Fiedler V., Grönholm T., Hellen H., Herrmann E., Jalonen R., Jussila. M., Komppula M., Kosmale M., Plauškaite K., Reis R., Savola N., Soini P., Virtanen S., Aalto P., Del Masi M., Hakola H., Keronen P., Vehkamäki H., Rannik Ü., Lehtinen K.E.J. & Hari P. 2004d. Aerosols in boreal forest: wintertime relations between formation events and bio-geo-chemical activity. *Boreal Env. Res.* 9: 63–74.

Kuparinen A. 2006. Mechanistic models for wind dispersal. *Trends in Plant Science* 11: 296–301.

Kuparinen A., Markkanen T., Riikonen H. & Vesala T. 2007a. Modeling air-mediated dispersal of spores, pollen and seeds in forested areas. *Ecological Modelling* 208: 177–188.

Kuparinen A., Snäll T., Vänska S. & O'Hara B.R. 2007b. The role of model selection in describing stochastic ecological processes. *Oikos* 116: 966–974.

Marchuk G.I. [Марчук Г.И.] 1982. [*Mathematical modeling in the environmental problems*]. Nauka, Moscow. [In Russian].

McMurry P.H. & Eisele F.L. 2005. Preface to topical collection on nucleation and growth in urban Atlanta. *J. Geophys. Res.* 110, D22S01, doi:10:1029/2005JD006644.

Mårtensson E.M., Nilsson E.D., de Leeuw G., Cochen L.H. & Hansson H.-C. 2003. Laboratory simulations of the primary marine aerosol production. *J. Geophys. Res.* 108: 4297, doi:10.1029/2002JD002263.

Monahan E.C., Spiel D.E. & Davidson K.L. 1986. A model of marine aerosol generation via whitecaps and wave disruption. In: Monahan E.C. & MacNiochaill G. (eds.), *Oceanic whitecaps*, D. Reidel, Norwell, Mass., pp. 167–193.

Mäkelä J.M., Koponen I.K., Aalto P. & Kulmala M. 2000. Modal structure of number size distribution of ambient submicron particles at a boreal forest site. *J. Aerosol Sci.* 31: 595–611.

Pirjola L., Tsyro S., Tarrasón L. & Kulmala M. 2003. A monodisperse aerosol dynamics module, a promising candidate for use in long-range transport models: box model tests. *J. Geophys. Res.* 108, doi:10.1029/2002JD002867.

Prank M., Sofiev M., Kaasik M., Ruuskanen T., Kukkonen J. & Kulmala M. 2008. The origin and formation mechanics of aerosol during a measurement campaign in Finnish Lapland, evaluated using the regional dispersion model SILAM. In: Borrego C. & Miranda A.I. (eds.), *Air pollution modeling and its application XIX*, NATO Science for Peace and Security Series C, Environmental Security, Springer, Dordrecht, pp. 530–538.

Rannik Ü., Markkanen T., Raittila J., Hari P. & Vesala T. 2003. Turbulence statistics inside and over forest: influence on footprint prediction. *Boundary-Layer Meteorology* 109: 163–189.

Ruuskanen T.M., Kaasik M., Aalto P.P., Hõrrak U., Vana M., Mårtensson M., Yoon Y., Keronen P., Mordas G., Nilsson D., O'Dowd C., Noppel M., Alliksaar T., Ivask J., Sofiev M., Prank M. & Kulmala M. 2007. Concentrations and fluxes of aerosol particles during LAPBIAT measurement campaign in Värriö field station. *Atmos. Chem. Phys.* 7: 3683–3700.

Saarikoski S., Sillanpää M., Sofiev M., Timonen H., Saarnio K., Teinilä K., Karppinen A., Kukkonen J. & Hillamo R. 2007. Chemical composition of aerosols during a major biomass burning episode over northern Europe in spring 2006: experimental and modelling assessments. *Atmos. Environ.* 41: 3577–3589.

Seinfeld J.H. & Pandis S.N. 2006. *Atmospheric chemistry and physics*. John Wiley & Sons, New Jersey.

Siljamo P., Sofiev M., Severova E., Ranta H., Kukkonen J., Polevova S., Kubin E. & Minin A. 2008. Sources, impact and exchange of early-spring birch pollen in the Moscow region and Finland. *Aerobiologia* 24: 211–230.

Skjøth A.C., Sommerw J., Stachz A., Smithz M. & Brandt J. 2007. The long-range transport of birch (*Betula*) pollen from Poland and Germany causes significant pre-season concentrations in Denmark. *Clinical and Experimental Allergy* 37: 1204–1212.

Sogacheva L., Dal Maso M., Kerminen V.-M. & Kulmala M. 2005. Probability of nucleation events and aerosol particle concentration in different air mass types arriving at Hyytiälä, southern Finland, based on back trajectory analysis. *Boreal Env. Res.* 10: 479–491.

Sogacheva L., Hamed A., Facchini M.C., Kulmala M. & Laaksonen A. 2007. Relation of air mass history to nucleation events in Po Valley, Italy, using back trajectories analysis. *Atmos. Chem. Phys.* 7: 839–853.

Sofiev M. 2000. A model for the evaluation of long-term airborne pollution transport at regional and continental scales. *Atmos. Environ.* 34: 2481–2493.

Sofiev M.A., Gusev A.V. & Lenhart L. 1996. Experimental study of the sensitivity of the long-range air pollution transport model to the temporal resolution of emission data. In: Borrell P.M., Borrell P., Cvitas T., Kelly K. & Seiler W. (eds.), *Proceedings of EUROTRAC Symposium'96*, Computational Mechanism Publications, Southampton, pp. 667–673

Sofiev M., Siljamo P., Ranta H. & Rantio-Lehtimäki A. 2006a. Towards numerical forecasting of long-range air transport of birch pollen: theoretical considerations and a feasibility study. *Int J. Biometeorol.* 50: 392–402.

Sofiev M., Valkama I., Fortelius C. & Siljamo P. 2006b. Forward and inverse modelling of radioactive pollutants dispersion after Chernobyl accident. In: Borrego C. &

Renner E. (eds.), *Air pollution modelling and its applications XVIII*, Elsevier, Amsterdam, pp. 283–292.

Sofiev M., Siljamo P., Valkama I., Ilvonen M. & Kukkonen J. 2006c. A dispersion modelling system SILAM and its validation against ETEX data. *Atmos. Environ.* 40: 674–685.

Sofiev M., Jourden E., Kangas L., Karvosenoja N., Karppinen A. & Kukkonen J. 2006d. Numerical modelling of the spatial distribution of fine particulate matter in Europe and Finland. *Report Series in Aerosol Science* 83: 348–353.

Stern R., Builtjes P., Schaap M., Timmermans R., Vautard R., Hodzic A., Memmesheimer M., Feldmann H., Renner E., Wolke R. & Kerschbaumer A. 2008. A model intercomparison study focussing on episodes with elevated PM10 concentrations. *Atmos. Environ.* 42: 4567–4588.

Tammet H., Mirme A. & Tamm E. 2002. Electrical aerosol spectrometer of Tartu University. *Atmos. Res.* 62: 315–324.

Tunved P., Hansson H.-C., Kerminen V.-M., Ström J., Dal Maso M., Lihavainen H., Viisanen Y., Aalto P.P., Komppula M. & Kulmala M. 2006. High natural aerosol loading over boreal forests. *Science* 312: 261–263.

Unden P. (ed.) 2002. *HIRLAM5 scientific documentation*. HIRLAM Project, SMHI, Norrkoping, Sweden.

Vana M., Kulmala M., Dal Maso M., Horrak U. & Tamm E. 2004. Comparative study of nucleation mode aerosol particles and intermediate air ions formation events at three sites. *J. Geophys. Res.* 109, D17201, doi:10.1029/2003JD004413.

Vehkamäki H., Dal Maso M., Hussein T., Flanagan R., Hyvärinen A., Lauros J., Merikanto J., Mönkkönen P., Pihlatie M., Salminen K., Sogacheva L., Thum T., Ruuskanen T., Keronen P., Aalto P.P., Hari, P., Lehtinen K.E.J., Rannik Ü. & Kulmala M. 2004. Atmospheric particle formation events at Värriö measurement station in Finnish Lapland 1998–2002. *Atmos. Chem. Phys.* 4: 2015–2023.

Vesala T., Kljun N., Rannik Ü., Rinne J., Sogachev A., Markkanen T., Sabelfeld K., Foken Th. & Leclerc M.Y. 2008. Flux and concentration footprint modeling: state of the art. *Environ. Pollut.* 152: 653–666.

Vira J. 2008. *Variational data assimilation in chemistry-transport modeling*. M.Sc. thesis, University of Helsinki.